CrossMark

ORIGINAL PAPER

Synthesis of a nanocomposite of organo-montmorillonite/cellulose-g-poly(methyl methacrylate) by atom-transfer radical polymerization and its application in removal of 2,4-dichlorophenol

Ronglan Wu · Lingyuan Tian · Wei Wang

Abstract We report a study on the synthesis of cellulose-g-poly(methyl methacrylate)/organo-montmorillonite and its application in the removal of 2,4-dichlorophenol (2,4-DCP) from aqueous solution. The nanocomposite of cellulose-g-PMMA/OMMT was synthesized by using atom transfer radical polymerization. We investigated the effects of four reaction parameters on the grafting efficiency and percentage. The nanocomposite was characterized by Fourier transform infrared spectroscopy, thermogravimetric analysis, X-ray diffraction, transmission electron microscopy and scanning electron microscopy. The effects of four parameters on the adsorption of 2,4-DCP were studied, which included pH, grafting percentage, adsorbate weight and the initial concentration of 2,4-DCP. Furthermore, adsorption isotherms and kinetics were investigated.

Introduction

The demand for quality water has increased along with concerns about public health and the environment (Haworth 1990). Disposal sewage requires purification before discharge into the environment (Demirbas 2009). This calls for the development of wastewater treatment technologies (Gadipelly et al. 2014). Adsorption has long been used for wastewater treatment because of its low cost and feasibility (O'Connell et al. 2008). Agricultural byproducts, such as cellulose, are broadly applied as adsorbents because of the large reserves (Sahu et al. 2013), but there are many disadvantages of byproducts directly attained from plants. For example, neat celluloses are biodegradable, and the physicochemical properties are not as stable as those of modified celluloses (Uschanov et al. 2011; Man et al. 2015a, b). Moreover, the waste-adsorbing capacity is quite weak (Amin et al. 2006). Thus, a large adsorption capacity and stable physicochemical properties have been the focus in the field of wastewater treatment. These can be achieved by chemical modification of cellulose or doping with other materials (Chen 2004).

R. Wu · W. Wang (✉)
Key Laboratory of Oil and Gas Fine Chemicals, Department of Chemistry, Xinjiang University, Ürümqi 830046, China
e-mail: wei.wang@kj.uib.no

L. Tian
CPI YILI Energy Chemical Group Co., Ltd., Huocheng Coal-Gas Branch, Yili, Xinjiang 835200, China

W. Wang
Department of Chemistry and Centre for Pharmacy, University of Bergen, 5007 Bergen, Norway

Heavy metal ions and phenols are common pollutants in sewage. The weak adsorption capacity of neat cellulose is due to the lack of a special interaction between the cellulose and pollutants. This can be improved by the chemical modification of cellulose, e.g., using grafting monomers that possess functional groups that interact with such compounds in sewage. In one of our previous studies, this idea was proven by grafting different types of monomers that can effectively interact with these two types of pollutants (Wu et al. 2015).

The justification of doping inorganic materials rests on the enhancement of the physicochemical properties of cellulose (Chen et al. 2008). These inorganic materials include carbon nanotubes, graphite oxide, titania and clays, etc. Among clays, montmorillonite (MMT) is of particular interest because of its lamellar structure. Modified cellulose can intercalate or exfoliate the MMT layers, resulting in a homogeneous distribution of MMT in a nanocomposite. The nanocomposite formed of MMT and cellulose exhibits great mechanical and thermal stability (Mahmoudian et al. 2012). Therefore, in the present study, we intended to combine these two strategies to synthesize a thermostable nanocomposite of cellulose possessing a high adsorption capacity. We used organo-MMT as a template for cellulose and modified cellulose by grafting methyl methacrylate to enhance the adsorption toward phenols.

Materials and methods

Materials

Natural cellulose (bamboo pulp) was purchased from Beiyan Yasong Paper Co. (Chengdu, China) with 650 degrees of polymerization as measured using an Ubbelohde viscometer in a cupriethylenediamine hydroxide solution. 2-Bromoisobutyryl bromide (2-BiB), N,N,N',N'',N''-pentamethyldiethylenetriamine (PMDETA), copper(I) bromide (CuBr), 2,4-dichlorophenol (2,4-DCP) and allyl chloride were purchased from Aladdin Industrial Corp. (Shanghai, China). Methyl methacrylate (MMA), N,N-dimethylformamide (DMF), acetone and other organic solvents were purchased from Tianjing Chemical Corp. (Tianjing, China). Montmorillonite was purchased from Huawei Bentonite Group Co., Ltd. (Weifang, China). The stock solutions of HCl and NaOH with 0.1 mol/l

concentration were prepared to adjust the pH of solutions. The chemicals were used as received, and Milli-Q water with a resistivity of 18 MΩ cm was used in all experiments. An ionic liquid, 1-allyl-3-methylimidazolium chloride, was used to dissolve cellulose, and to synthesize the ionic liquid we followed a previously reported procedure (Wu et al. 2015).

Synthesis of organo-montmorillonite (OMMT)

Organo-montmorillonite was prepared by following the same method as reported in a previous study (Praus et al. 2006). Montmorillonite was dispersed in a solution of water/ethanol (1:1, v/v). Cetyltrimethylammonium bromide was added to the suspension. The mixture was warmed up to 70 °C in a water bath and ultrasonicated for 24 h. The suspension was filtered and washed thoroughly with water in order to remove bromide ions. The residue was dried at 70 °C for 48 h.

Synthesis of OMMT/cellulose-g-PMMA by ATRP

Synthesis of the cellulose initiator (cellulose-BiB)

Cellulose (0.2 g) was added to the ionic liquid, 1-allyl-3-methylimidazolium chloride (10.0 g). The suspension was warmed up to 80 °C and stirred until the cellulose was dissolved. The solution was removed from the heating source to let it gradually cool down to room temperature. Afterwards, the solution was put in an ice bath for 15 min, and bromoisobutyryl bromide was added to the solution at a weight ratio of 5:1 to cellulose. The solution was stirred for 30 min and then warmed to 50 °C for 2 h. The mixture was poured into a large amount of water. The precipitate was collected and thoroughly washed with water. The precipitate was dried at 50 °C for 24 h.

Synthesis of OMMT/cellulose-g-PMMA

Cellulose-BiB (0.135 g) was added to 15 ml acetone with a certain amount of PMDETA (see the "Results" section). The solution was degassed by a freeze-pump-thaw cycle and refilled with nitrogen. The procedure was repeated two more times. CuBr was added under nitrogen flow, and the flask with the solution was vacuumed again and refilled with nitrogen. This

procedure was repeated twice. Then the mixture of MMA and OMMT was added to the solution under nitrogen. The freeze-pump-thaw procedure was repeated three times. The solution was warmed to 70 °C and maintained at 70 °C for 6 h. When the reaction was finished, the product was put into 1 mol/l HCl solution. A precipitate formed and was washed thoroughly to remove the copper ions and unreacted monomers.

Optimum ATRP conditions

The optimum reaction condition can be evaluated by the grafting efficiency (GE) and grafting percentage (GP). They are calculated as follows:

$$GE = \frac{W_2 - W_0}{W_1} \tag{1}$$

$$GP = \frac{W_2 - W_0}{W_0} \tag{2}$$

where W_0, W_1 and W_2 represent the weights of the neat cellulose, monomer and grafted cellulose, respectively. Following the aforementioned procedure, we investigated the effects of four reaction parameters on GP and GE. These four parameters were the molar ratio of the monomer (MMA) to the initiator, molar ratio of the catalyst to the ligand, temperature and weight ratio of OMMT. The effects of these parameters on GE were also investigated by using an orthogonal experimental design. The results of the orthogonal experiments are presented in the supporting information.

Characterization

Fourier transform infrared spectroscopy (FTIR) measurements were carried out on an IR Prestige-21 (Shimadzu, Japan). The samples were dried in a vacuum overnight and mixed with KBr to compress them into KBr pellets. The measurements were performed at wavenumbers from 400 to 4000 cm^{-1}. The micrograph of cellulose, grafted cellulose and OMMT/cellulose-g-PMMA was captured on a transmission electron microscope (TEM) (JEM 2100, Japan) and scanning electron microscope (SEM) (Leo 1430VP, Germany). Thermogravimetric analysis (TGA) was carried out on a Q600SDT TGA instrument (TA Instruments Inc.). Temperature scanning was performed in the range of

30–500 °C with a scanning rate of 5 °C/min. X-ray diffraction (XRD) measurements were carried out on a Focus D8 diffractometer (Bruker, Germany). The patterns with Cu kα radiation ($\lambda = 1.5418 \mathring{A}$) were recorded in the region of 2θ from 1° to 15° with a step speed of 0.02°/s.

Adsorption experiments

A series of 2,4-DCP solutions with various concentrations was prepared by using a stock solution of 2,4-DCP with the concentration of 2 g/l. Standard solutions of 2,4-DCP were prepared and measured by UV-Vis spectroscopy (Shimadzu FTAS-990, Japan) to draw a standard curve. The wavelength used here was 284 nm. A 25-ml aliquot of 2,4-DCP solution was mixed with 0.035 g of the absorbent in a vial. The vial was mounted in a shaking water bath for 2 h. A small portion of supernatant was removed from the container to measure the concentration of 2,4-DCP. The amount (q_e) of the solute adsorbed per gram of the adsorbent at equilibrium was calculated as follows:

$$q_e = \frac{c_0 - c_e}{W} V \tag{3}$$

where c_0 and c_e are the concentrations of the solute before and after adsorption, respectively; W represents the weight of the adsorbent; V represents the volume. The influence of various parameters on adsorption was evaluated, including the pH, initial concentration of the adsorbate, weight of the adsorbent and GP of the nanocomposite. All the adsorption experiments were conducted three times to ensure the reproducibility.

Adsorption isotherm

The adsorbent (0.035 g) was mixed with a 25.00-ml aliquot of 2,4-DCP solution in a vial. Five samples were prepared in parallel. The vials were mounted in a water bath and shaken for 2 h at five temperatures. The absorbance of 2,4-DCP in the supernatant was measured at the wavelength of 284 nm and then converted to its concentration. The adsorbed amount was calculated using Eq. 3.

Adsorption kinetics

The adsorbent (0.035 g) was mixed with a 500-ml aliquot of 2,4-DCP solutions in a vial. Four samples

were prepared with different concentrations of 2,4-DCP. A portion of the 0.05 ml supernatant was removed to measure the absorbance. The adsorbed amount was calculated using Eq. 3.

Results and discussions

The results contain three parts, organized as follows: (1) effects of the four reaction conditions on the yield of the final product; (2) characterization of the nanocomposite (OMMT/cellulose-g-pMMA); (3) results of the adsorption experiments, including the optimum conditions of the adsorption, adsorption isotherms and kinetics.

Effects of the ATRP reaction conditions on GE and GP

The four reaction conditions of OMMT/cellulose-g-PMMA were investigated, including the temperature, molar ratio of PMDETA to CuBr, weight ratio of OMMT to MMA and molar ratio of MMA to cellulose-BiB. The results are presented in Fig. 1. Without specific indications, the reaction conditions are given as follows: the temperature was 70 °C; the reaction time was 6 h; the molar ratio of MMA to cellulose-BiB was 200:1; the molar ratio of PMDETA to CuBr was 2:1; the weight ratio of OMMT to MMA was 0.015. In each experiment, only one parameter was changed, and the effect of the parameter was investigated.

Figure 1a exhibits the effects of the reaction temperature on GP and GE. The polymerization was performed in the temperature regime of 30–80 °C. As presented in Fig. 1a, GP and GE increase with temperature. At 30 and 40 °C, GP and GE are nearly zero. Abrupt increases of GE and GP are found between 50 and 60 °C. This indicates that the reaction is initialized at temperatures higher than 40 °C. Above 70 °C, the effect of temperature is not significant. However, based on the mechanism of ATRP, the optimal temperature depends on monomers and catalysts. Higher activation energy has a major effect on the radical propagation than on the radical termination, which may lead to better control of monomer conversion. In this reaction, the optimum temperature is chosen to be 70 °C with regard to the volatile solvent used in the polymerization.

In Fig. 1b, we present the results of the effects of the molar ratio of [PMDETA]/[CuBr] on GP and GE. GE is a parameter essentially evaluating the monomer conversion. The results in Fig. 1b indicate that the monomer conversion increases with the molar ratio of [PMDETA]/[CuBr]. At a molar ratio of [PMDETA]/[CuBr] higher than 2, the curve levels off. A further increase of the molar ratio has a minor effect on the monomer conversion. The maxima of GP and GE were obtained at [PMDETA]/[CuBr] = 2/1. The structure formed by the catalyst and ligand generally depends on the solvent used in the reaction (Nanda and Matyjaszewski 2003). The catalyst and ligand complex should not affect the monomer conversion if the polymerization has been provided with sufficient time.

Figure 1c exhibits the effects of the weight ratio of OMMT to MMA on GP and GE. As shown in Fig. 1c, both GP and GE decrease when the ratio is above 1.5. This result can be understood as follows. GP and GE are highly dependent on the monomer concentration. When the monomer concentration decreases, we would expect decreases of GP and GE. However, increases of GP and GE were observed when the ratio was less than 1.5, which we are not yet able to interpret. In Fig. 1a–c, the curves of GP and GE overlap. This is because the molar ratio of [MMA] to [cellulose] was kept constant in the first three experiments.

The effects of the molar ratio of [MMA] to [cellulose-BiB] on GE and GP are presented in Fig. 1d. Due to the change of the molar ratio of [MMA] to [cellulose], the GP and GE curves no longer overlap. A linear increase is observed for GP as expected, while a maximum value is found for the curve of GE, which appears at the molar ratio of 200. The value of GE is found slightly above 80 % when [MMA]:[cellulose-BiB] = 200. This means the percentage of monomer conversion is 80 %. A further increase of the monomer fraction would not render even greater conversion of the monomer. Based on the results obtained in this section, the optimum parameters to prepare cellulose-g-PMMA/OMMT are as follows: the temperature is 70 °C; the reaction time is 6 h; the molar ratio of [PMDETA] to [CuBr] is 2:1; the molar ratio of [MMA] to [cellulose-BiB] is 200:1; the weight ratio of OMMT to MMA is 1.5 wt%. These reaction conditions were used to prepare the nanocomposite in the rest of the experiments.
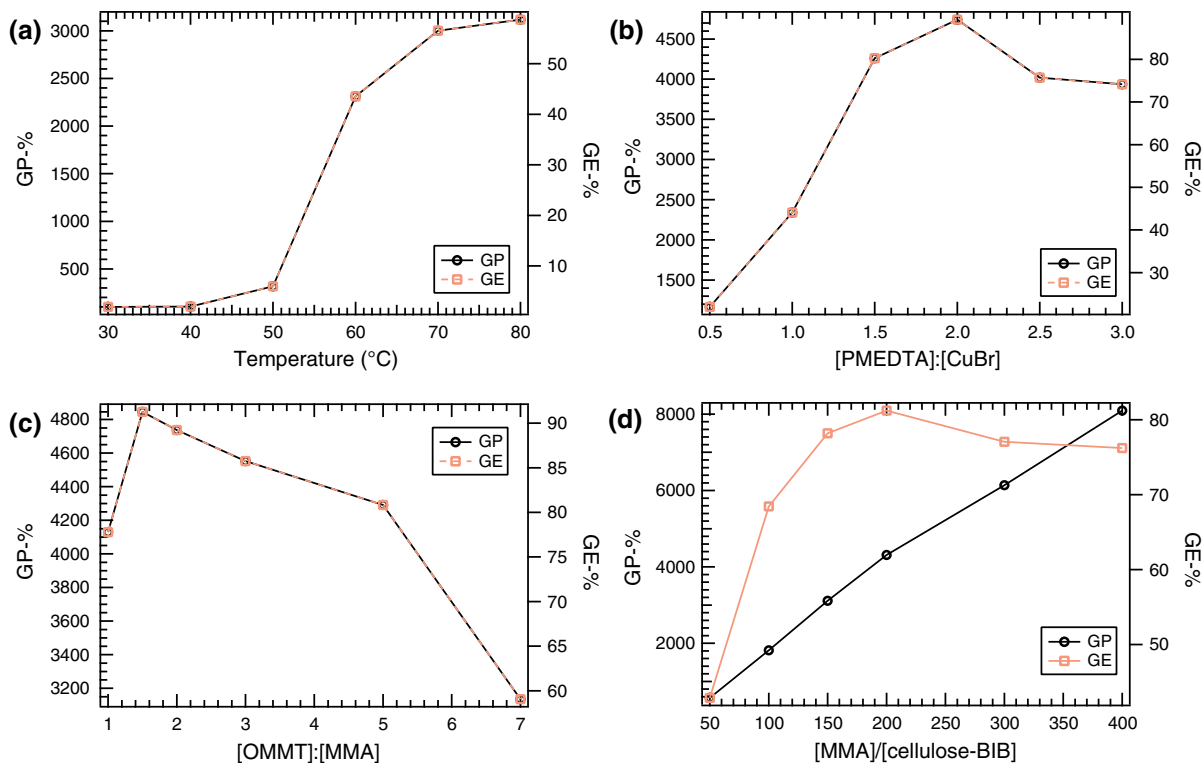
Fig. 1 Effects of the reaction parameters on GP and GE, which include **a** the temperature, **b** molar ratio of PMDETA/CuBr, **c** weight ratio of OMMT/MMA and **d** molar ratio of MMA/cellulose-BiB

Characterization of OMMT/cellulose-g-PMMA

Fourier transform infrared (FTIR) spectra

The FTIR spectra of neat cellulose, MMT, OMMT, cellulose-BiB and cellulose-g-PMMA/OMMT are presented in Fig. 2. The infrared spectrum of neat cellulose shows a strong and broad absorption at $3443 \, cm^{-1}$ due to the stretched vibration of hydrogen-bounded hydroxyl groups. The spectrum of MMT exhibits two characteristic absorption peaks at 518 (Si–O) and $463 \, cm^{-1}$ (Mg–O) (Tahir and Amin 2013). The spectrum of OMMT exhibits two characteristic peaks at 2851 and $2922 \, cm^{-1}$, differing from the spectrum of MMT, which may be attributed to the antisymmetric and symmetric vibration peaks of the methyl groups. This indicates the cations on MMT have been substituted by cetyltrimethylammonium (CTA^{+}). For the spectrum of cellulose-BiB, the absorption at $3443 \, cm^{-1}$ decreases substantially. Four characteristic absorption peaks are observed at 1732 (stretching vibration of C=O), 1451 (in plane C–H

stretching vibrations), 1050 and $1149 \, cm^{-1}$ (antisymmetric and symmetric vibration peaks of ester groups) (Liu et al. 2008). The spectrum of cellulose-g-PMMA/OMMT contains the same characteristic absorption peaks as those in the spectrum of cellulose-BiB (1732, 1451, 1272 and $1149 \, cm^{-1}$); moreover, it exhibits the characteristic absorption peaks of OMMT (518 and $463 \, cm^{-1}$).

Scanning electron microscopy (SEM) and transmission electron microscopy (TEM)

The morphologies of neat cellulose, cellulose-BiB, OMMT and cellulose-g-PMMA/OMMT were characterized by scanning electron microscopy (SEM), and the morphologies of the latter two were also characterized by transmission electron microscopy (TEM). The SEM and TEM images are presented in Figs. 3 and 4, respectively. The cellulose morphology was substantially changed after the reaction with bromoisobutyryl bromide, and the difference can be observed by comparing Fig. 3a and b. In Fig. 3b, some
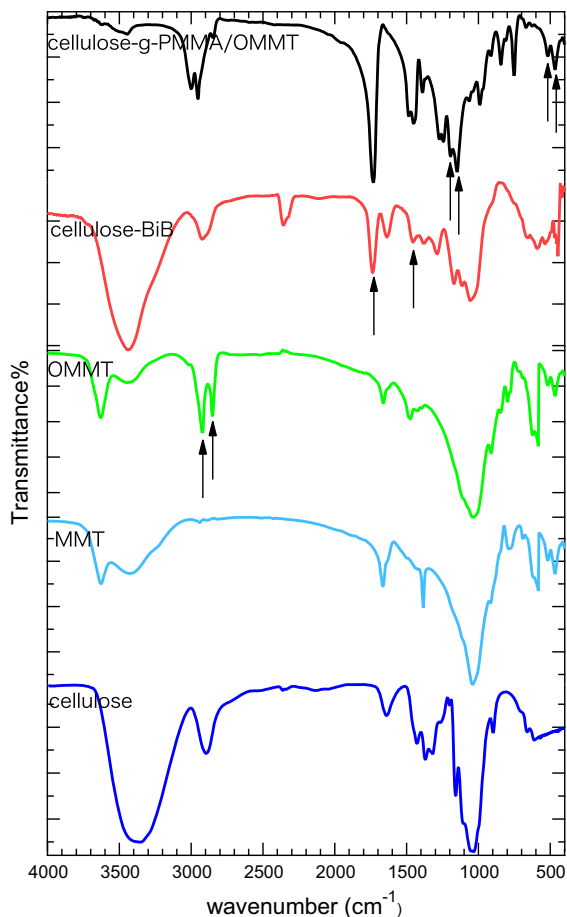
Fig. 2 FTIR spectra of neat cellulose, MMT, OMMT, cellulose-BiB and cellulose-g-PMMA/OMMT

aggregates with high contrast can be observed on the cellulose surface. This is caused by the reaction with bromoisobutyryl bromide, which brings in hydrophobic groups on the cellulose chains. Figure 3c presents the surface morphology of OMMT where the layer structure is clearly observed. Some layers are exfoliated, while most preserve the multilayer structure, which indicates that mostly intercalation occurs. The layer structure of OMMT can be better observed in Fig. 4a. The surface morphology of cellulose-g-PMMA/OMMT is presented in Fig. 3d. In Fig. 3d, the layered structure of OMMT cannot be observed in the nanocomposite, and the nanocomposite morphology is transformed to a porous structure. This structure is often desired in adsorption materials because of the large surface area. The TEM image of the nanocomposite is presented in Fig. 4b. The layer structure of OMMT cannot be observed in the TEM image.

OMMT is embedded in organic materials, and the nanocomposite morphology becomes difficult to capture with TEM.

X-ray diffraction (XRD)

The XRD patterns of MMT, OMMT and cellulose-g-PMMA/OMMT are presented in Fig. 5. The characteristic diffraction peaks (001) of MMT and OMMT can be found at $2\theta = 7°$ and $4.8°$, respectively. By applying Bragg's law, the minimum distances between layers are calculated to be 1.2 nm for MMT and 1.8 nm for OMMT. The loss of the (001) peak in the XRD trace of cellulose-g-PMMA/OMMT may be attributed to the exfoliation of the OMMT layers as observed in both Figs. 3 and 4.

Thermogravimetric analysis (TGA)

The TGA results of cellulose, MMT, OMMT, cellulose-BiB and cellulose-g-PMMA/OMMT are presented in Fig. 6. The weight loss at 100 °C is due to dehydration for all samples. The onset of decomposition of neat cellulose is at 275 °C, and the sample is totally decomposed at 345 °C. The residue is about 31 % of the initial weight. After cellulose reacts with BiB, the thermostability decreases, as shown in Fig. 6. The onset of the decomposition of cellulose-BiB is at 220 °C, and at 415 °C the remaining weight is about 16.8 %. For MMT, the weight loss is substantially low because of its inorganic nature. The intercalation of CTA^+ leads to a decrease of the thermostability as expected. The onset of decomposition starts at 315 °C. At 500 °C, and the residue is about 64 %, which suggests the weight percentage of CTA^+ in the OMMT equals approximately 25 %. The thermostability of cellulose-g-PMMA/OMMT increases, especially at the temperatures above 250 °C.

Adsorption of 2,4-DCP on cellulose-g-PMMA/OMMT

In this section, 2,4-DCP is used as a model pollutant to exhibit the adsorption capacity of cellulose-g-PMMA/OMMT. We evaluated the effects of four factors on the adsorption of 2,4-DCP, including the adsorbent weight ($W_{adsorbent}$), initial concentration of adsorbate (c_0), pH and grafting percentage (GP). Afterwards, the
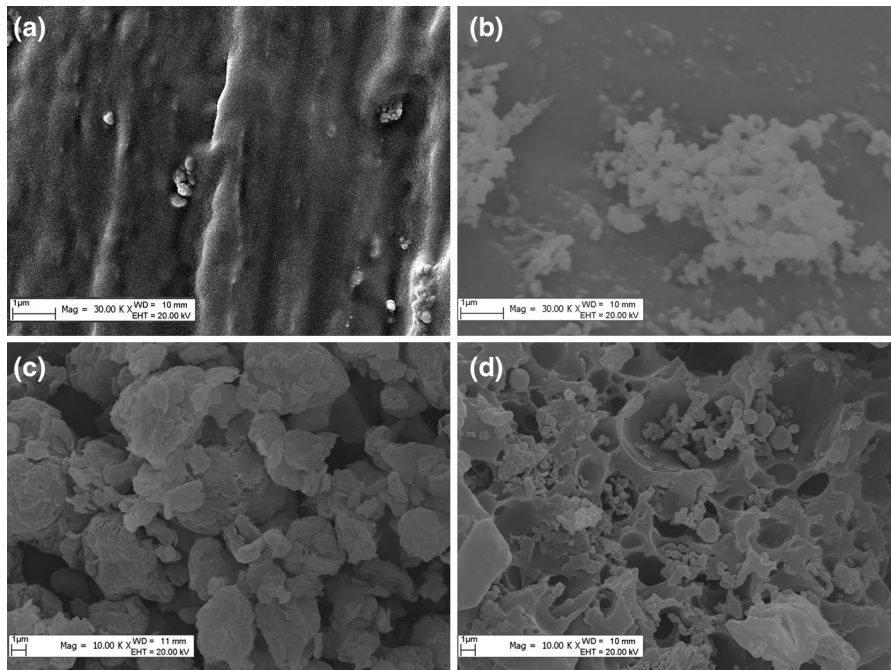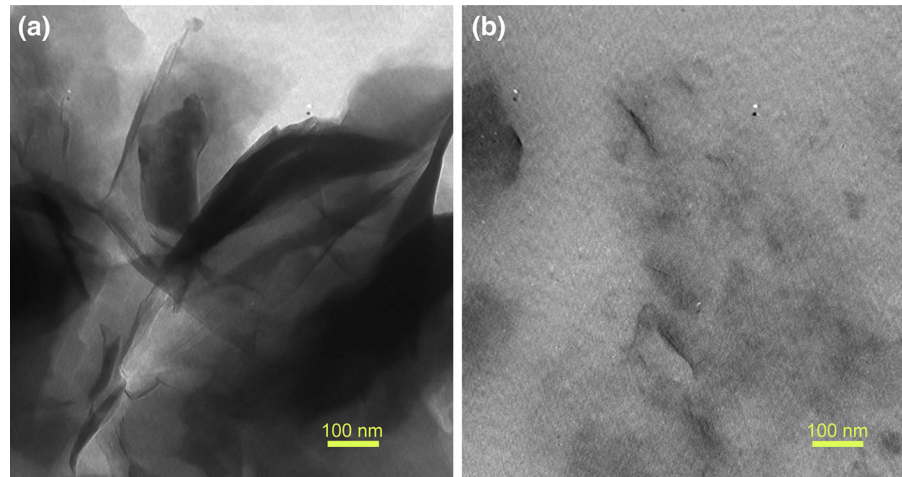
Fig. 3 SEM images of **a** neat cellulose, **b** cellulose-BiB, **c** OMMT and **d** cellulose-g-PMMA/OMMT

Fig. 4 TEM images of **a** OMMT and **b** cellulose-g-PMMA/OMMT

adsorption experiments were performed at five temperatures in order to draw the adsorption isotherms. In the last part, the kinetics of the adsorption were investigated at four initial concentrations of 2,4-DCP.

Influence of $W_{adsorbent}$, c_0, pH and GP on adsorption

The effects of four parameters on the adsorption were evaluated, and the results are presented in Fig. 7. In these experiments, adsorption was performed with the following conditions: the initial concentration of 2,4-DCP was 0.2 g/l; the GP of the polymer was 7000 %; the adsorbent weight was 1.60 g/l; the time and temperature were 2 h and 3 °C, respectively. In each experiment, only one parameter was changed. The adsorbed amount per gram of the adsorbent is presented as a function of the parameter.
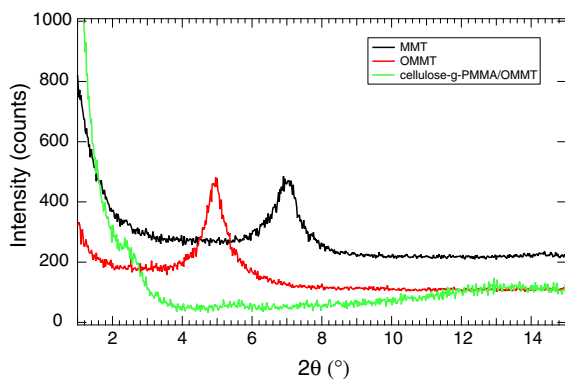
Fig. 5 XRD spectra of **a** MMT, **b** OMMT and **c** cellulose-g-PMMA/OMMT
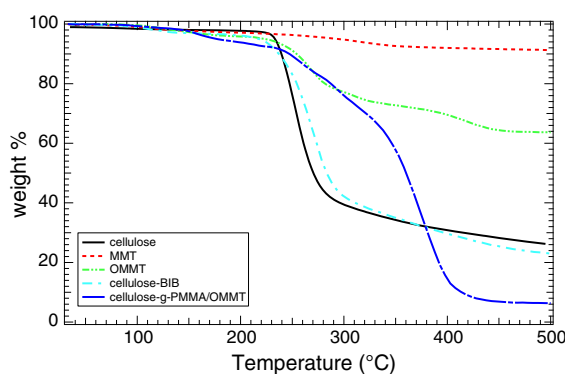

Fig. 6 Thermogravimetric analysis of neat cellulose, MMT, OMMT, cellulose-BiB and cellulose-g-PMMA/OMMT

In Fig. 7a, the effect of the adsorbent weight is presented. It is clearly observed that q_e decreases with the adsorbent weight. This is because the initial concentration of 2,4-DCP is far below the saturation of the adsorption. As to the effect of the initial concentration of 2,4-DCP, q_e increases linearly with c_0, as presented in Fig. 7b. The line in Fig. 7b is a linear regression of the result.

The influence of pH on the adsorbed amount is presented in Fig. 7c. The pH value is often an important factor in adsorption because of the charge properties of the adsorbent and thus the mechanism of adsorption. In the current study, the pH value of the solution affected the ionization of both 2,4-DCP and OMMT and further affected the adsorption caused by electrostatic and hydrophobic interactions. In Fig. 7c, the adsorbed amount increases in both strongly acidic and weakly alkaline environments, while the absolute change of the adsorbed amount is not significant.

Moreover, no particular trend is shown in Fig. 7c; therefore, we will not discuss it further.

The adsorbed amount is presented as a function of GP in Fig. 7d. The result interestingly exhibits that the adsorbed amount decreases with GP, even though the decreased amount is not significant. We believe that GP is an important factor because the binding site increases with GP. However, as shown in Fig. 7d, the result indicates the grafting percentage is not essential with respect to the adsorption of 2,4-DCP. This may be attributed to the addition of OMMT to the nanocomposite, which also adsorbs 2,4-DCP. The relative amount of OMMT may decrease with the increase of GP.

Adsorption isotherm

The adsorption experiments were performed at five temperatures with five initial concentrations of 2,4-DCP. The experiments were carried out to determine the adsorption isotherms. We tried to fit the results to both the Langmuir and Freundlich isotherms, and better regression was achieved using the Freundlich isotherm. Thus, only the Freundlich isotherm is presented here. In Fig. 8, the logarithm of q_e is presented as a function of the logarithm of the equilibrium concentration (c_e). The lines in Fig. 8 are the results of linear regression based on the Freundlich isotherm:

$$\log q_e = \log k_F + \frac{\log c_e}{n} \tag{4}$$

where c_e represents the concentration of 2,4-DCP at equilibrium, k_F represents the Freundlich constant, and n is a constant at a certain temperature. The results of the linear regression are presented in Table 1. The free energy was calculated using the following equation:

$$\Delta G = -RT\ln\left(\frac{c_0 - c_e}{c_e}\right), \tag{5}$$

where R represents the gas constant and T the temperature. Due to the empirical nature of the Freundlich isotherm, we were not able to obtain other thermodynamic parameters, such as the enthalpy and entropy of adsorption (Baierlein 2001).

The three parameters shown in Table 1 exhibit a consistent trend in which each parameter has a minimum at 313 K and increases at both lower and higher temperatures. For ΔG, this indicates that the
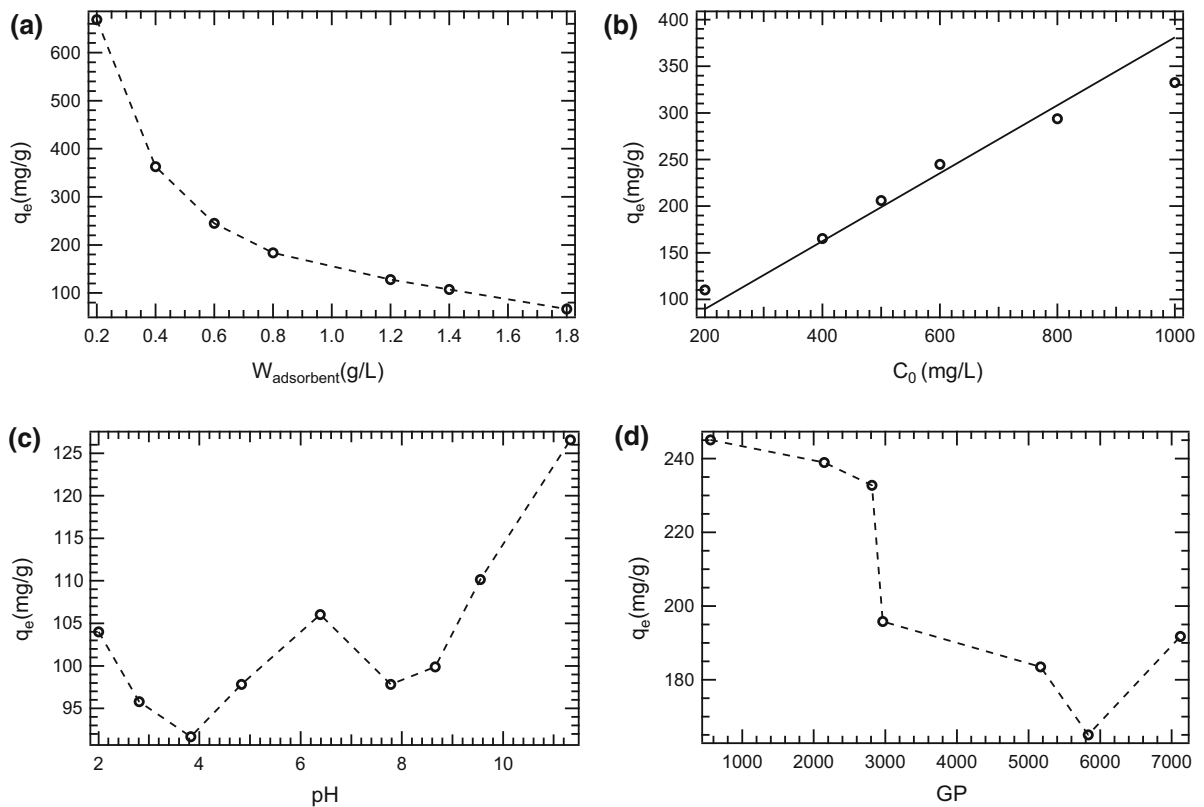
Fig. 7 Effects of **a** the adsorbent weight, **b** initial concentration of 2,4-DCP, **c** pH and **d** grafting percentage on the adsorbed amount per gram of cellulose-g-PMMA/OMMT
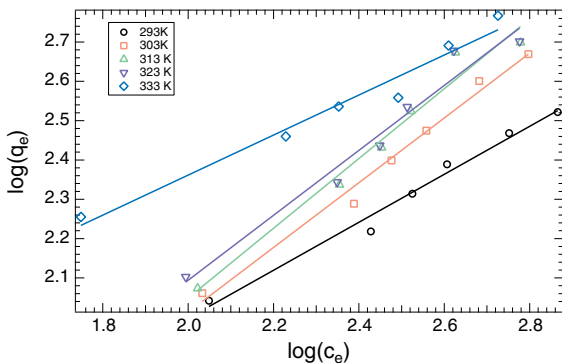

Fig. 8 Freundlich isotherms of the adsorption of 2,4-DCP on cellulose-g-PMMA/OMMT within the temperature regime of 293–333 K

Table 1 Thermodynamic parameters for the adsorption of 2,4-DCP on cellulose-g-PMMA/OMMT

Temperature (K)	k_F	n	ΔG
293	5.98	1.63	−14.57
303	2.23	1.21	−5.62
313	1.88	1.13	−4.89
323	2.77	1.21	−7.44
333	11.89	1.61	−32.92

adsorption of 2,4-DPC is more favorable at a low or high temperature, while the adsorption becomes less favorable at 313 K. The adsorption between PMMA and 2,4-DCP is mainly caused by a hydrophobic interaction (Wu et al. 2015). In this case, the binding of 2,4-DCP on cellulose-g-PMMA is endothermic, which is consistent with the results showing that increasing temperature leads to a decrease of ΔG, while at low temperatures the adsorption also becomes favorable. We assume that this is due to the adsorption on OMMT.

Adsorption kinetics

The adsorption kinetics were investigated at four initial concentrations of 2,4-DCP. The adsorption kinetics are usually described with models, such as pseudo-first order adsorption, pseudo-second order adsorption or the diffusion model. In the previous study, we found that the adsorption of 2,4-DCP occurs mostly on the cellulose surface (Wu et al. 2015). It could be well described by the pseudo-second order model of adsorption; therefore, the same model was applied here. The kinetics results are presented in Fig. 9. In the figure, t/q_t is plotted against time as the pseudo-second order model can be represented in a linear form as follows:

$$\frac{t}{q_t} = \frac{1}{k_2 q_e^2} + \frac{t}{q_e} \tag{6}$$

where t is the time of adsorption; q_t is the adsorbed amounts at time t; k_2 is a rate constant that is dependent on both the temperature and initial concentration of the adsorbate. As presented in Fig. 9, the data show good compliance with the model. The results obtained from the linear regression are presented in Table 2 and show that the amount adsorbed at equilibrium increases with the initial concentration of 2,4-DCP; however the adsorption rate decreases with the initial concentration. The values of q_e obtained by the pseudo-second order model can be used for comparison with the values of the experimental results presented in Fig. 7b. We find the values of q_e calculated from the model are larger than the results in Fig. 7b, especially at high concentrations. This
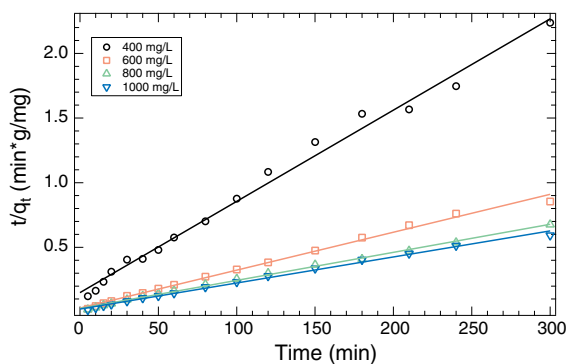
Table 2 Parameters in the pseudo-second order model obtained by linear regression as presented in Fig. 9

c_0 (mg/l)	q_e (mg/g)	k_2 (l/min)
400	139	0.340
600	338	0.336
800	456	0.208
1000	492	0.207

result may indicate that q_e predicted by using the pseudo-second order model is suitable for cases when the adsorbate is at low concentration (Ho 2006).

Conclusions

Cellulose-g-PMMA/OMMT was synthesized by using ATRP. The effects of four reaction conditions on the grafting percentage and grafting efficiency were evaluated. Based on the yield, we obtained the optimum condition to perform polymerization. The nanocomposite of cellulose-g-PMMA/OMMT was characterized using FTIR, XRD and TGA, and the results provided the structure of cellulose-g-PMMA in OMMT. The TEM, SEM and XRD results showed that the lamellae of OMMT are rather exfoliated during the polymerization. The morphology of the nanocomposite was captured by SEM and TEM. The nanocomposite of cellulose-g-PMMA/OMMT was utilized to remove 2,4-DCP in aqueous solution. The effects of pH, GP, the adsorbent weight and initial concentration of 2,4-DCP on the adsorption were studied. The results suggest that q_e decreases with adsorbent weight and GP, while it increases with the initial concentration of 2,4-DCP. The effect of pH on q_e is more complex in that q_e is low at a pH of around 4 and 8, but high at strongly acidic and alkaline conditions. In addition, the adsorption isotherms were obtained by studying the adsorption at five temperatures. The data were interpreted using the Freundlich isotherm. The kinetics of the adsorption behave as pseudo-second adsorption. The rate constant decreases with the initial concentration of 2,4-DCP.

Fig. 9 Pseudo-second order adsorption kinetics of 2,4-DCP on cellulose-g-PMMA/OMMT. The temperature for conducting the experiments is 303 K

References

Amin MN, Kaneco S, Kitagawa T, Begum A, Katsumata H, Suzuki T, Ohta K (2006) Removal of arsenic in aqueous solutions by adsorption onto waste rice husk. Ind Eng Chem Res 45(24):8105–8110

Baierlein R (2001) The elusive chemical potential. Am J Phys 69(4):423–434

Chen B (2004) Polymer-clay nanocomposites: an overview with emphasis on interaction mechanisms. Br Ceram Trans 103(6):241–249

Chen B, Evans JRG, Greenwell HC, Boulet P, Coveney PV, Bowden AA, Whiting A (2008) A critical appraisal of polymer-clay nanocomposites. Chem Soc Rev 37:568–594

Demirbas A (2009) Agricultural based activated carbons for the removal of dyes from aqueous solutions: a review. J Hazard Mater 167(1–3):1–9

Gadipelly C, Pérez-González A, Yadav GD, Ortiz I, Ibáñez R, Rathod VK, Marathe KV (2014) Pharmaceutical industry wastewater: review of the technologies for water treatment and reuse. Ind Eng Chem Res 53(29):11571–11592

Haworth A (1990) A review of the modelling of sorption from aqueous solution. Adv Colloid Interface Sci 32(1):43–78

Ho Y-S (2006) Review of second-order models for adsorption systems. J Hazard Mater 136(3):681–689

Liu C, Zhang Y, Huang J (2008) Well-defined star polymers with mixed-arms by sequential polymerization of atom transfer radical polymerization and reverse addition-fragmentation chain transfer on a hyperbranched polyglycerol core. Macromolecules 41(2):325–331

Mahmoudian S, Wahit MU, Ismail A, Yussuf A (2012) Preparation of regenerated cellulose/montmorillonite nanocomposite films via ionic liquids. Carbohydr Polym 88(4):1251–1257

Man X, Wu R, Jiang X, Xu S, Wang W (2015a) Organomontmorillonite supported titania nanocomposite synthesized by using poly(methyl methacrylate) grafted cellulose as template and its application in photodegradation. Cellulose. 22:3189–3198

Man X, Wu R, Lv H, Wang W (2015b) Synthesis of a montmorillonite-supported titania nanocomposite with grafted cellulose as a template and its application in photocatalytic degradation. J Appl Polym Sci 132(41):42627

Nanda AK, Matyjaszewski K (2003) Effect of [pmdeta]/[cu(i)] ratio, monomer, solvent, counterion, ligand, and alkyl bromide on the activation rate constants in atom transfer radical polymerization. Macromolecules 36(5):1487–1493

O'Connell DW, Birkinshaw C, O'Dwyer TF (2008) Heavy metal adsorbents prepared from the modification of cellulose: a review. Bioresour Technol 99(15):6709–6724

Praus P, Turicová M, Študentová S, Ritz M (2006) Study of cetyltrimethylammonium and cetylpyridinium adsorption on montmorillonite. J Colloid Interface Sci 304(1):29–36

Sahu GC, Garg A, Majozi T, Bandyopadhyay S (2013) Optimum design of waste water treatment network. Ind Eng Chem Res 52(14):5161–5171

Tahir M, Amin NS (2013) Photocatalytic reduction of carbon dioxide with water vapors over montmorillonite modified TiO2 nanocomposites. Appl Catal B Environ 142–143:512–522

Uschanov P, Johansson L-S, Maunu S, Laine J (2011) Heterogeneous modification of various celluloses with fatty acids. Cellulose 18(2):393–404

Wu R, Tian L, Wang W, Man X (2015) Bifunctional cellulose derivatives for the removal of heavy-metal ions and phenols: synthesis and adsorption studies. J Appl Polym Sci 132(17):41830